

# Evaluation of Different Topographic Parameters Extracted from the Digital Elevation Measurements with the Use of Geostatistical Interpolation Methods

Fahmy F. F. Asal

Civil Engineering Department, Faculty of Engineering, Menoufia University, Shebin El-Kom, Egypt  
Email: fahmy.asal@sh-eng.menofia.edu.eg

**How to cite this paper:** Asal, F.F.F. (2023) Evaluation of Different Topographic Parameters Extracted from the Digital Elevation Measurements with the Use of Geostatistical Interpolation Methods. *International Journal of Geosciences*, 14, 1226-1242. <https://doi.org/10.4236/ijg.2023.1412062>

**Received:** November 3, 2023

**Accepted:** December 26, 2023

**Published:** December 29, 2023

Copyright © 2023 by author(s) and Scientific Research Publishing Inc. This work is licensed under the Creative Commons Attribution International License (CC BY 4.0).

<http://creativecommons.org/licenses/by/4.0/>



Open Access

## Abstract

Gradient slope, aspect slope, profiling and contourlines are important topographic parameters that can be derived from digital elevation data obtained from different sources with exploitation of different interpolation techniques. Geostatistical interpolation methods such as ordinary kriging models constitute reliable alternatives to deterministic approaches in creation of continuous surface models from discrete elevation data. This research aimed at extraction, analysis, and evaluation of different terrain parameters elevation measurements with the use of different ordinary kriging models including the linear model, the circular model, the spherical model, the exponential models, and the Gaussian model. Different ordinary kriging models under ESRI ArcView 3.3 package along with its 3D analyst and Spatial analysis extensions have been exploited in extraction of gradient slope maps, aspect slope maps, and hillshade maps in addition to contourline maps from a sample of elevation data. Visual analysis of the gradient slope maps shows great similarities between the slope maps from the linear, circular, spherical, and exponential OK models, however, that from OK Gaussian models look very different as different sizes and arrangements of the colour patches, referring to different tones and different textures where smooth tones and smooth textures dominate the gradient slope map from the OK Gaussian model. Thus, gradient slope degradation and smoothing are considerably high in the gradient slope map from Gaussian model compared to the slope maps from the other four OK models. Also, the mean slope in the Gaussian model records the lowest value with the lowest value of the standard deviation of slopes in the same map reflecting less structured and highly smoothed gradient slope map compared to the slope maps from the other OK models. Thus, similar sizes of the colour patches and similar tones and similar texture dominate the different

---

aspect slope maps. This is not the case in **Figure 2(e)** which depicts the aspect slope map extracted with the use of the Gaussian OK model where the smooth colour patches, smooth tones and smooth textures can be observed. Also, the Aspect map, hillshade map and the contourline map from Gaussian OK model are visually and statistically different from their corresponding maps created with the other four OK models. Finally, analysis of extracted two groups of profiles shows that the profiles extracted with the use of linear, circular, spherical, and exponential OK models run close and show highly corrugated and varied terrain. This is different from the profiles with the use of the Gaussian model which are less corrugated and tend to smooth and approximate different parts of the terrains.

### Keywords

Topographic Parameters, Gradient Slope, Aspect Slope, Shaded Relief, Contourline, Profiling, Ordinary Kriging Models

---

## 1. Introduction

Gradient slope, aspect slope, shaded relief, profile curvature, contourline curvature and drainage networks represent important topographic parameters or in other words terrain parameters that are usually employed in studying a wide range of engineering and environmental problems [1] [2]. Gradient slope, aspect slope shaded relief, contourline curvature and profile curvature are considered important topographic parameters as they are not only efficient in describing the structure of the topography of the Earth's surface, but also, are exploited as vital parameters in land use planning, hydrological modelling, landslide monitoring in addition to soil erosion analysis [3] [4] [5]. Topographic parameters are extracted from digital elevation data, so they are expected to contain an error budget part of it is the errors inherited from the original digital elevation data in addition to that part of errors created by the interpolation algorithms exploited in creation of the different topographic parameters [2] [5] [6] [7]. The accuracy of the different topographic parameters extracted from different types and different sources of the digital elevation data sets depends on some factors such as: the source of the data, the techniques employed in collecting the data, the density of data, the interpolation methods employed in creation of continuous surfaces from the digital elevation data in addition to the structure of the elevation data whether it is a grid model, a contour map, a Triangular Irregular Network (TIN) model, ...etc. Additionally, the accuracy of the extracted topographic parameters depends on the horizontal resolution and the vertical precision at which the elevation data is represented, the topographic complexity of the landscape and finally it depends on the interpolation algorithms exploited in creation of the different topographic parameters [8].

Due to developments in computing technologies, geostatistical techniques have been integrated with GIS and become strong alternatives to deterministic me-

thods in interpolation of spatial data and creation of continuous surface models. In addition, application of the statistical approaches in the analysis of the interpolated layers provides strength to the interpolation operations with the use of the geostatistical methods [9]. In this context two main types of geostatistical kriging interpolation methods may be distinguishable: the Ordinary Kriging (OK) and the Universal Kriging (UK). Chaplot *et al.* (2006) [10] state that kriging interpolation methods including Ordinary Kriging interpolation, and Universal Kriging are examples of geostatistical interpolation techniques. Also, they state that Kriging interpolation approaches are geostatistical methods that take into consideration the distance and the degree of variation between known data points.

To quantify the spatial variation in the input digital elevation data, the semi-variogram of the sample data is estimated where semivariogram is one of the most essential tools in geostatistical analyses to quantify and model the spatial variability degree of data. These semivariogram models can later be used to make estimations with the use of other geostatistical approaches including kriging, cokriging, ...etc. [11] [12]. Interpolations of DEM elevations with kriging are performed through steps. The first step encompasses fitting a model which means creation of the variograms and covariance functions for estimation of the statistical dependence, referred as spatial autocorrelation values depending on the model of autocorrelation [13]. The second step involves making an estimation of the unknown values [13] [14]. In Ordinary Kriging (OK) the first step is to create a semivariogram from the scatter elevation data set to be interpolated where semivariogram consists of an empirical experimental variogram in addition to a model of a semivariogram. As a clarification, a semivariogram can be defined as a mathematical model of the semivariance expressed as a function of lag while displaying the statistical correlation of nearby points in addition to spatial autocorrelation referring to feature similarity based on feature locations and feature values simultaneously [15]. Ordinary Kriging (OK) assumes that the variation in z-values is free of any structural component/drift. Thus, ordinary kriging can be performed through the application of different five models on the digital elevation data set. The five OK models may be distinguishable as: linear OK model, circular OK model, spherical OK model, exponential OK model, and Gaussian OK model. These five different ordinary kriging models are presented as follows [16] [17]:

1) Linear Model:

$$\gamma(h) = \begin{cases} A_0\delta(h) + A_1h & \text{for } h < a \\ A_0 + A_1a & \text{for } h \geq a \end{cases} \quad (1)$$

2) Circular Model:

$$\gamma(h) = \begin{cases} \frac{A_0\delta(h)}{\pi} + \frac{w}{\pi} \left[ \frac{h}{a} \sqrt{1 - \left(\frac{h}{a}\right)^2} - \arcsin\left(\frac{h}{a}\right) \right] & \text{for } h < a \\ A_0 + w & \text{for } h \geq a \end{cases} \quad (2)$$

3) Spherical Model:

$$\gamma(h) = \begin{cases} A_0\delta(h) + \frac{w}{2} \left[ \frac{3h}{a} - \left(\frac{h}{a}\right)^3 \right] & \text{for } h < a \\ A_0 + w & \text{for } h \geq a \end{cases} \quad (3)$$

4) Exponential Model:

$$\gamma(h) = A_0\delta(h) + w \left[ 1 - \exp\left(-\frac{h}{a}\right) \right] \quad (4)$$

5) Gaussian Model:

$$\gamma(h) = A_0\delta(h) + w \left[ 1 - \exp\left(-\frac{h}{a}\right)^2 \right] \quad (5)$$

where:  $\gamma(h)$  = the semivariogram for the elevation variable  $h$ .

$\delta(h) = 1$  for  $h > 0$ ;  $\delta(h) = 0$  for  $h = 0$ .

$A_0$  = nugget effect caused by possible errors of measurement;

$A_1$  = the rate of decrease of the spatial covariance in the field for the linear model;

$A_0 + w$  = sill, which is the variance of the field less the discontinuity  $A_0$ ;

$a$  = range, or the correlation distance, and is in practice the maximum distance for which observations are correlated.

Ordinary kriging with a spherical model where parameters are to be determined by weighting least squares methods are commonly used to fit semivariogram models. Thus, the advantage of this method is the statistical formulation of the best linear unbiased estimate. However, the disadvantage of that method could be that the weights must be computed for each node of the grid, that is why this method is usually used for small samples where Ordinary Kriging approaches could produce undesirable “pits” and “circular” contours [18] [19].

This research aims at extraction of different topographic parameters from ground surveying measurements with the use of different ordinary kriging models including linear model, circular model, spherical model, exponential model, and Gaussian model. In addition, evaluation and comparative analysis of the different extracted topographic parameters including gradient slope maps, slope aspect maps, hillshade maps, contourline maps and terrain profiles created from the test data with the use of different OK models constitute main objectives of this research.

## 2. Research Data and Methodology

A sample of ground surveying elevation data collected from a construction site in Cairo, Egypt has been employed in this study. The elevation data represents a test site of corrugated terrain. The sample data consists of about 3000 spot elevation measurements forming a density of one spot elevation measurement for every 211.119 squared meters and an average spacing between successive spot elevation measurements of less than 15.0 meters. The minimum elevation in the

sample data records 116.73 m while the maximum elevation depicts 138.57 m and the above the mean sea level. Thus, a range of elevations of about 21.84 m can be computed in the digital elevation data set. Additionally, the median elevation depicts 129.62 meters while the mode elevation gives 131.96 meters. Finally, the mean elevation calculates 128.763 m while the standard deviation of elevations in the sample data is  $\pm 4.325$  m, referring to highly varied and corrugated terrains.

Different ordinary kriging models including the linear model, the circular model, the spherical model, the exponential model and the gaussian models have been used in extraction of the different topographic parameters from the sample of ground surveying data with use of the Environmental Systems Research Institute (ESRI) ArcView 3.3 package with 3D analyst and Spatial analysis extensions. Gradient slope maps, aspect slope maps, hillshade maps in addition to contourline maps have been extracted from the ground surveying elevation data with the employment of the different ordinary kriging models. The different extracted topographic parameters from different OK models have been subjected to comparative visual and statistical analyses. Moreover, groups of longitudinal and cross profile have been extracted from the digital elevation data sets with exploitation of the different OK models. The extracted groups of longitudinal and cross profiles have been presented and analyzed.

### 3. Extraction of Gradient Slope Maps from Ground Surveying Elevation Measurements

Terrain slope, known as slope gradient, is an important topographic parameter that is usually employed in representing the earth's surface for many applications including features extraction, analysis of terrain geomorphology and land use planning, [20]. Slope gradient referred to as the slope constitutes the angle  $G$  between the tangent plane  $P$  and the horizontal plane  $S$  at a given point of the topographical surface. Gradient slope is usually calculated using the following groups equation [8]:

$$\text{Slope} = \arctan \sqrt{p^2 + q^2} \quad (6)$$

where,

$$p = \frac{\partial z}{\partial x} \quad (7)$$

and

$$q = \frac{\partial z}{\partial y} \quad (8)$$

Slope values calculated from the application of Equations (6), (7), and (8) are obtained in degrees. However, some available software compute slope values of the terrain as percentages where a slope of 100% refers to a slope angle of  $45^\circ$  since  $\tan 45^\circ$  equals to 1 as the vertical difference between the elevations and the horizontal difference between the horizontal coordinates are equal.

Gradient slope maps have been created from the ground surveying digital elevation data set with the use of different ordinary kriging models including the linear model, the circular model, the spherical model, the exponential model, and the Gaussian model and depicted in **Figures 1(a)-(e)** respectively. Visual analysis based on investigating the elements of the digital image interpretation such as analysis of the shapes, sizes, 2D locations of the colour patches in the gradient slope maps is undertaken. Additionally, changes in the tones/colours within the gradient slope maps are investigated. Furthermore, the texture which expresses the arrangements and repetitions of the tones within the gradient slope map can be also evaluated as smooth, intermediate, or rough textures since this is one of the main digital image interpretation criteria [21]. Finally, studying the patterns within the slope maps from different OK models through analysis and evaluation of the arrangements of the spatial objects represent other is considered as important criteria of the elements of the digital image interpretation that should be examined [21] [22].

Visual analysis of the gradient slope maps in **Figure 1** shows clear similarities between the slope maps from the linear, circular, spherical, and exponential OK models **Figures 1(a)-(d)** respectively. This is clear in the similarities of the sizes, shapes, and arrangements of the corresponding colour patches within the different maps referring to similar tone variations and similar textures of the four

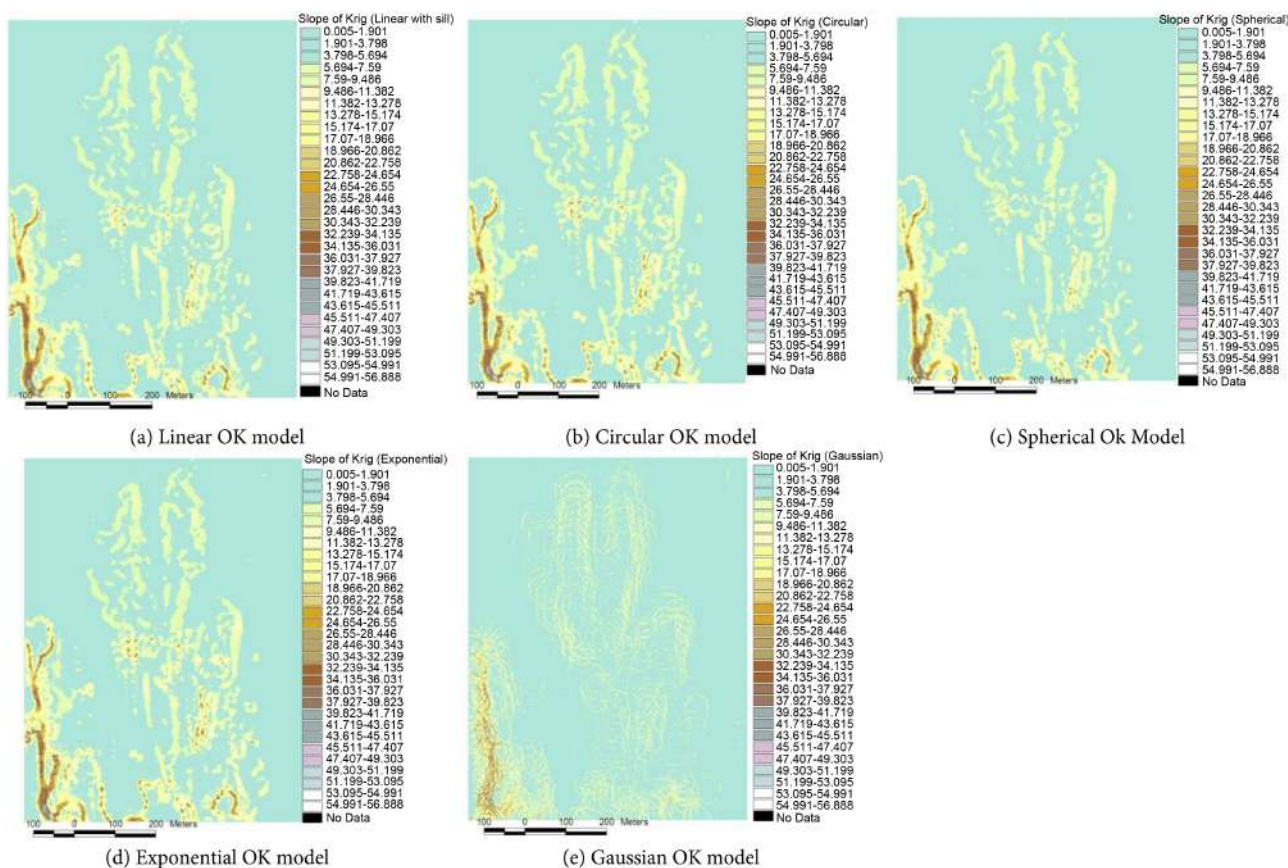


**Figure 1.** Gradient slope maps extracted from ground surveying measurements with employment of different OK models.

gradient slope maps. Also, the fore mentioned four gradient maps depict similar arrangement of the colour patches within the maps referring to great similarities of the patterns within these maps. On the other hand, the gradient slope map from OK Gaussian models looks very different from the gradient slope map from the other four OK models. This is very clear in the very different sizes of arrangement of the colour patches, referring to different tones and different textures where smooth tones and smooth textures dominate the gradient slope map from the OK Gaussian model. Also, the pattern in the gradient slope map from the OK Gaussian model is very different from the maps from the other four OK models. Furthermore, gradient slope degradation and smoothing is considerably high in the gradient slope map from Gaussian OK model compared to the slope maps from the other four OK models.

**Table 1** depicts the statistical properties of the gradient slope maps generated from the ground surveying digital elevation measurements through the employment of the different OK models namely, the linear model, the circular model, the spherical model, the exponential model and the Gaussian model. The linear model and circular models record high minimum values on the slopes compared to the other three OK models. This is not the case in the case of the maximum values where the spherical model records the lowest maximum value followed by the linear OK model, the circular OK model and the exponential models. However, the Gaussian model records the highest maximum value which is reflected on the highest value of the range of gradient slopes recorded

**Table 1.** Statistical analysis of the gradient slope maps extracted from ground surveying measurements with the use of different OK models.

OK Model	Linear kriging	Circular kriging	Spherical kriging	Exponential kriging	Gaussian kriging
No. of rows	857	857	857	857	857
No. of columns	681	681	681	681	681
Count	583,617	583,617	583,617	583,617	583,617
Minimum slope	0.00660	0.00623	0.00445	0.00536	0.00446
Maximum slope	51.19944	55.16736	49.90369	56.88752	60.97957
Range of slope	51.19284	55.16113	49.89924	56.88215	60.97511
Sum of slopes	2336869.68	2446700.19	2225205.41	2473394.30	1859760.81
Mean slope	4.0041152	4.1923045	3.8127837	4.2380436	3.1866118
Standard Deviation	4.79054	5.06692	4.51788	5.13766	4.15542

by the Gaussian OK model. When going to the values of the mean slopes Gaussian model records the lowest values of the mean elevations, the lowest values of the sum of slopes and the lowest value of the standard deviation of slopes. This supports the less structured and highly smoothed gradient slope map obtained from the Gaussian OK model interpreted from the visual analysis of the elements of the digital image interpretation. On the other hand, the gradient slope from the exponential model enjoys the highest values of the mean, the sum and the standard deviation of the gradient slopes. This refers to highly structured and less smooth gradient slope maps obtained from the OK exponential models.

#### 4. Extraction of Aspect Slope Maps with the Use of Different OK Models

Terrain aspect slope known as terrain aspect at any given point of the Earth's surface can be defined as the angle (A) in the clockwise direction measured from the north direction to the projection of the external normal (N) in the horizontal plane (H.). Terrain aspect slope is an important quantity that is employed in the determination of the measures of different important quantities that are crucial for different applications namely, insulation, temperature, vegetation, soil characteristics and moisture. Aspect slope is measured in degrees, where  $0^\circ$  is equal to North and  $180^\circ$  is equal to South [8] [23]. The extracted aspect slope maps in **Figure 2** are reclassified following dividing the 360 degrees of the horizon into quadrants and sub dials as shown in the legends.

Referring to **Figure 2** which depicts aspect slopes extracted from the ground surveying digital elevation data, great similarities between **Figures 2(a)-(d)** representing aspect slopes map created with the use of linear, circular, spherical and exponential OK models respectively. Thus, similar sizes of the colour patches and similar tones and similar texture dominate the four different aspect slope maps. This is not the case in **Figure 2(e)** which depicts an aspect slope map extracted with the use of the Gaussian OK model from the same digital elevation data where the smooth colour patches, smooth tones and smooth textures can be interpreted in that slope map.

**Table 2** records the statistical properties of the aspect slope maps generated with the use of different OK models. From **Table 2** it can be observed the aspect slope map from the Gaussian model records the highest values of the mean aspect slope and the highest aspect slope value of the standard deviation of the aspect slopes as well. This supports the outcomes from the visual analysis of the aspect slope maps.

#### 5. Analysis of Hillshade Maps Extracted from Ground Surveying Digital Elevation Data

Shaded relief known as hillshade constitutes an important topographic parameter and terrain derivative that provides visual representation of the terrain through supposed illumination of the surface at a defined direction and angle of

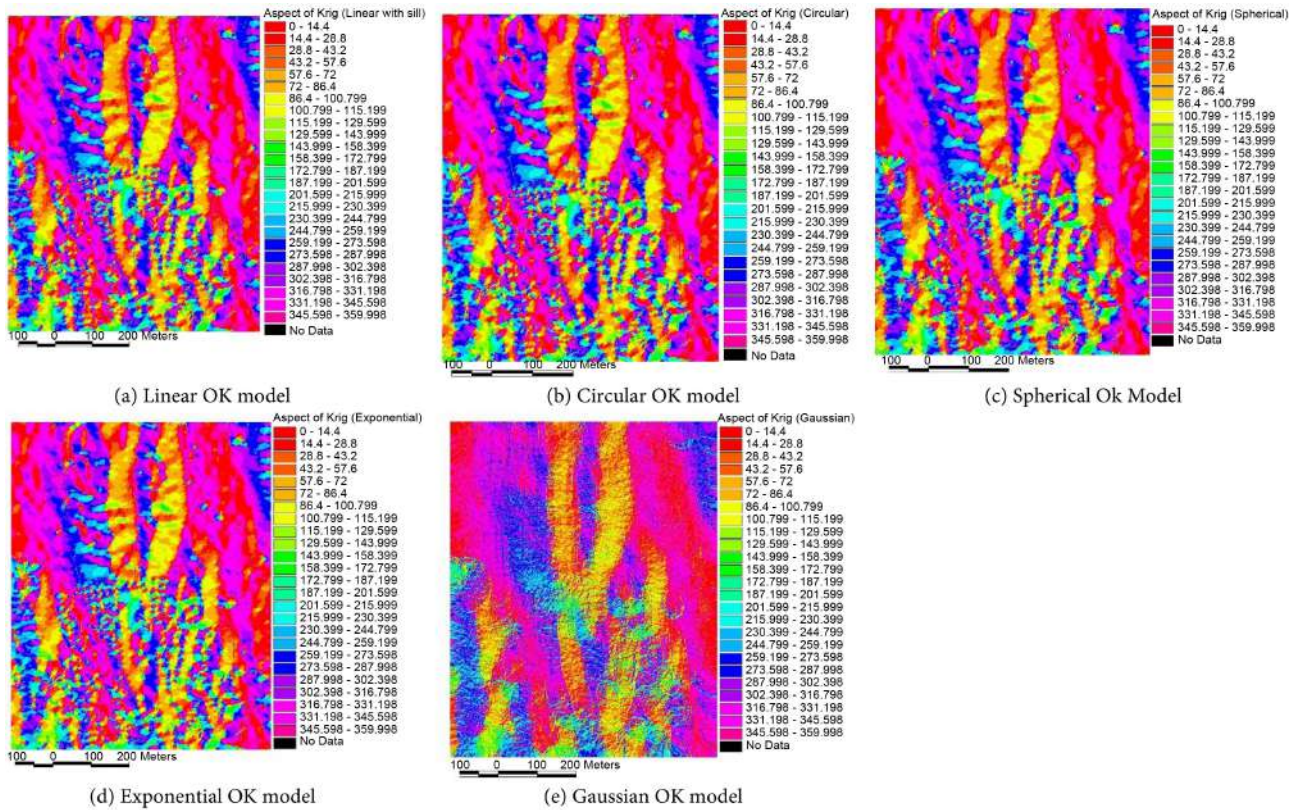


Figure 2. Aspect slope maps extracted from ground surveying measurements with the use of different OK models.

Table 2. Statistical properties of the aspect slope maps extracted from ground surveying measurements with the use of different OK models.

OK Model	Linear kriging	Circular Kriging	Spherical kriging	Exponential kriging	Gaussian kriging
No. of rows	857	857	857	857	857
No. of columns	681	681	681	681	681
Count	583,617	583,617	583,617	583,617	583,617
Min. aspect	0	0	0	0	0
Max. aspect	359.9979	359.9987	359.9984	359.9976	359.9987
Range of aspect	359.9979	359.9987	359.9984	359.9976	359.9987
Sum of aspect	115936848.4	115485665.6	116438817.9	115424744.2	117486081.4
Mean aspect	198.6523	197.8792	199.512382	197.774815	201.306818
Standard Deviation	127.1045	126.7913	127.4379	126.7014	127.4009

the light source. Before the invention of the digital computers, hillshade used to be examined manually through darkening of the different shaded areas on the map [8]. Maps of shaded terrains as if they are illuminated by a point light source referred to as hill-shading usually used in cartographic displays for representing

hilly parts of the terrains of rapid variations where hillshaded maps clarifies coarse landforms and fine texture terrains in addition to showing additional details [23]. In this analysis, visual analysis of the hillshaded maps **Figure 3** constitutes assessment of the elements of the digital image interpretation as explained in the previous sections. Visual analysis shows strong similarities between the hillshade maps in **Figures 3(a)-(d)** regarding sizes, shapes, and distribution of the colour patches. Also, the tones, textures, and patterns in the four hillshade maps are very close. This is not the case in **Figure 3(e)** which depicts a hillshade map created with the use of Gaussian model that is very different from the hillshade maps from the other four OK models. The tones and textures are very smooth compared to those in the other four models. Also, the pattern in **Figure 3(e)** is very different from the pattern in the other four hillshade maps.

**Table 3** presents the statistical properties of the hillshade maps extracted from the digital elevations data set through employment of the different models of the

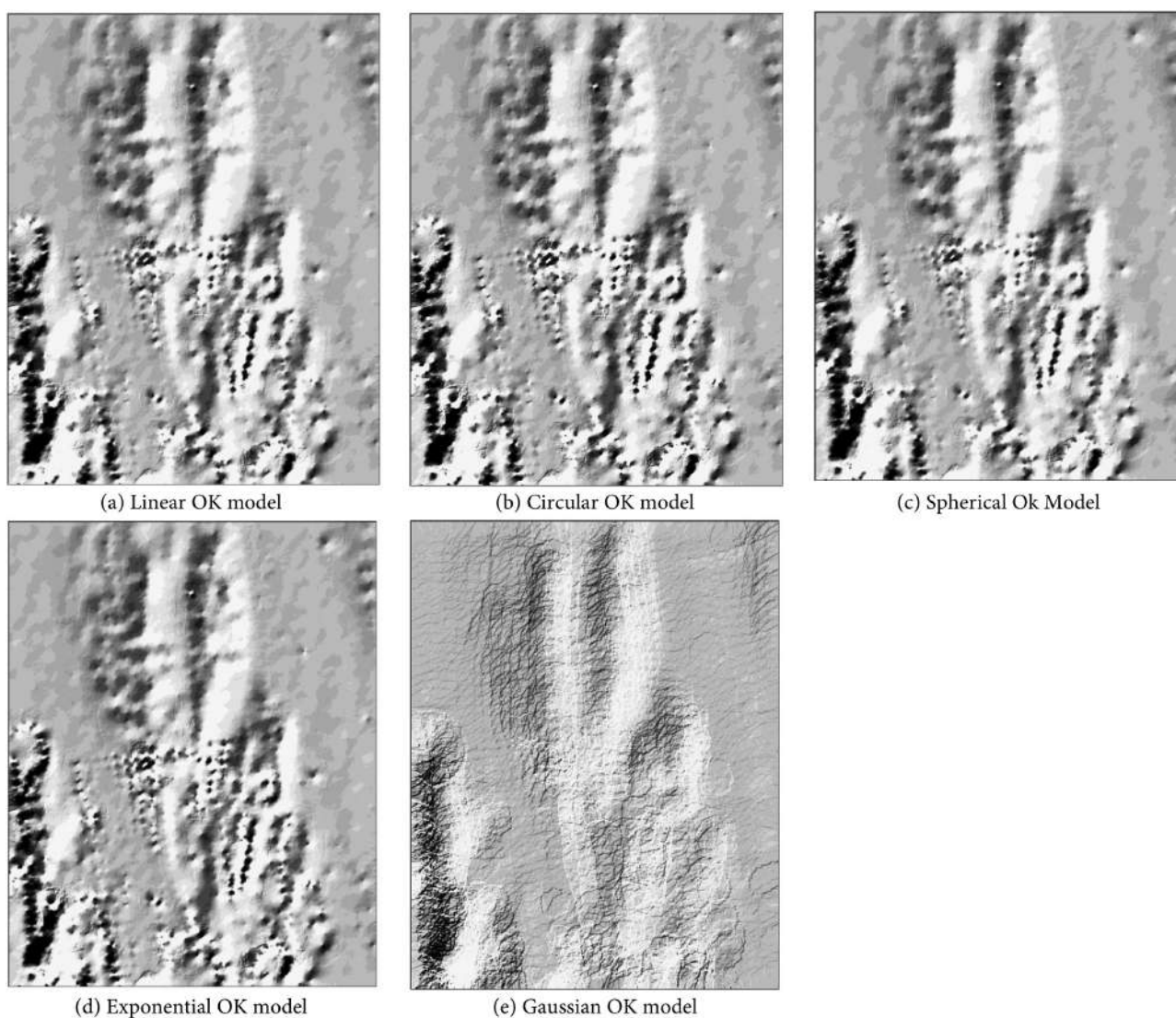


**Figure 3.** Hillshade maps extracted from ground surveying measurements with the use of different OK models.

**Table 3.** Statistical properties of the hillshade maps extracted from ground surveying measurements with the use of different ordinary kriging models.

OK Model	Linear	Circular	Spherical	Exponential	Gaussian
Statistical Quantity	OK	OK	OK	OK	OK
Rows	857	857	857	857	857
Cols	681	681	681	681	681
Count	580,545	580,545	580,545	580,545	580,545
Min	0	0	8	0	0
Max	254	254	254	254	254
Range	254	254	246	254	254
Sum	105196258.2	105126976.5	1105262758.3	105109242.0	105383587.0
Mean	181.2026	181.0833	181.3171	181.0527	181.5253
Standard Deviation	12.8221	13.6401	12.0272	13.8555	10.3045

OK geostatistical methods. From **Table 3**, the mean of the digital numbers in the hillshade from Gaussian model is higher than those from the other four models, however, the standard deviation from the Gaussian model is considerably lower than those of the hillshade maps from the other four models which refers to the high degree of smoothing the digital numbers and consequently smoothing of the hillshade from the Gaussian OK model.

## 6. Extraction of Contourline Maps from Ground Surveying Measurements with the Use of Different OK Models

Contourlines are important tools for representing, visualizing, and understanding the different spatial distribution of the different topographic elements of the terrain. Also, contourline maps are standard topographic products that are usually produced to provide clear understanding of the different terrain variations. The scale at which contourline map is extracted is very important as the system of contourlines under-represents the areas between the chosen intervals. Thus, if a contourline map is to be created from a raster Digital Terrain Model (DTM), then the vertical spacing between the successive contourlines that is known as the contour interval should be at least twice as the grid cell size of that DTM [8].

In this study, contourline maps have been created from the digital elevation data set with the use of OK models namely, linear, circular, spherical, exponential, and Gaussian models. Visual analysis of the contourline maps in **Figure 4** shows similarities between the contourline **Figures 4(a)-(d)** regarding contourline shapes, distribution and concentration of the contourlines all over the maps. The contourline map **Figure 4(e)** created with the use of the Gaussian model is visually different from the other four contourline maps, **Figures 4(a)-(d)**. This is

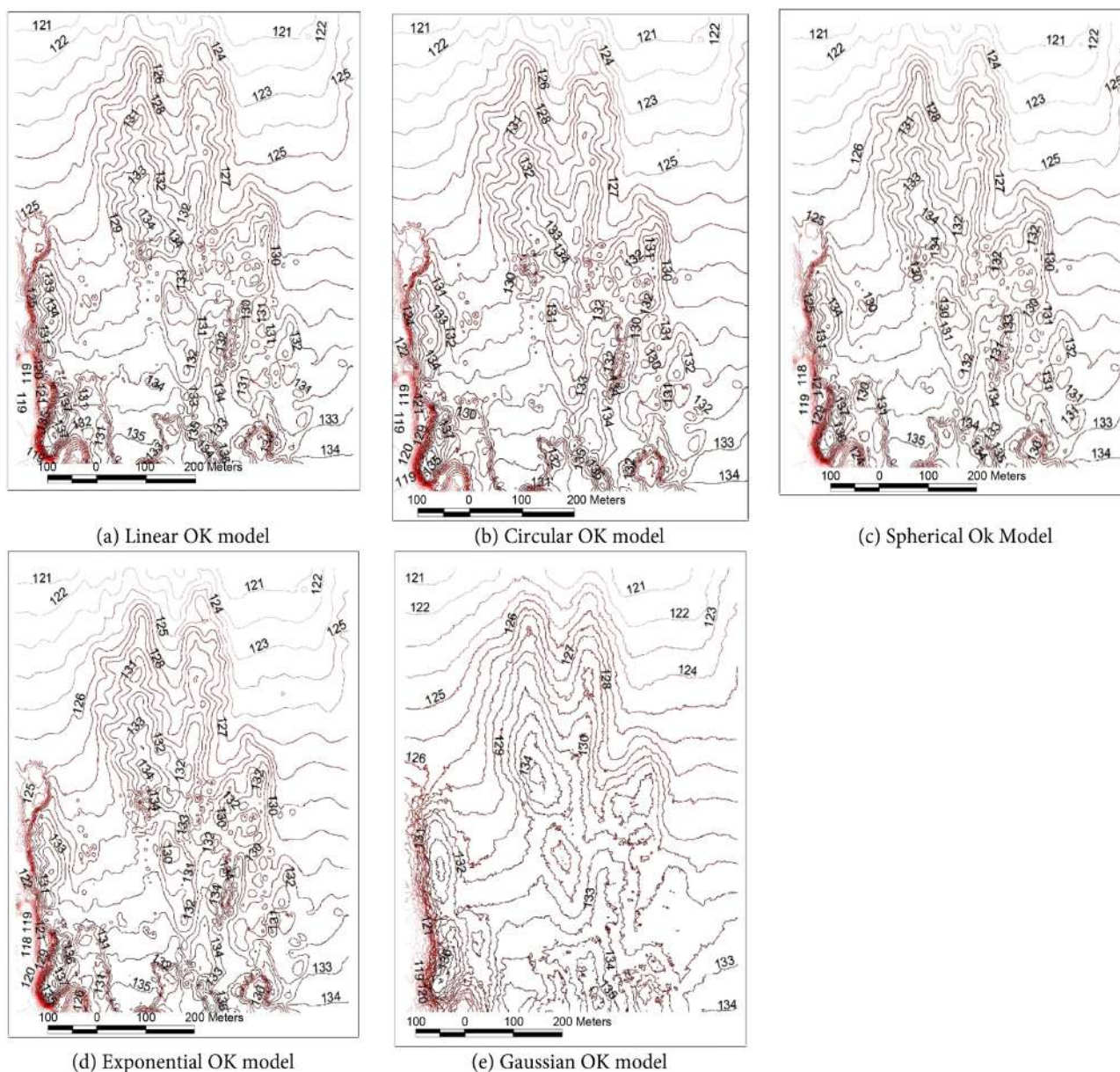


**Figure 4.** Contourline maps extracted from ground surveying measurements with the use of different OK models.

clear in the different shapes, different distribution, and different concentration of the contourlines compared to the other four contourline maps extracted from the linear, circular, spherical, and exponential OK models.

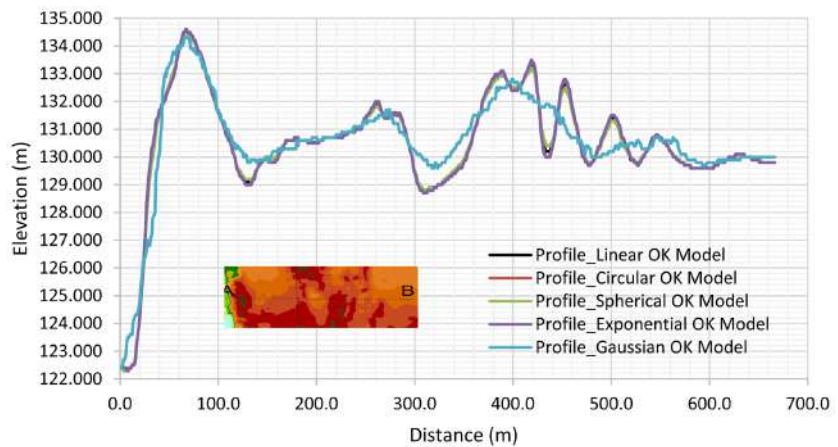
**Table 4** depicts the statistical properties of the four contourline maps depicted in **Figures 4(a)-(e)**. The statistical properties of contourline maps from linear, circular, spherical, exponential, and Gaussian OK models are close regarding the minimum contourline and the maximum contourline the mean contourline. However, regarding the standard deviation of the contourlines the Gaussian OK contourline map give the lowest standard deviation compared to the other four contourline. This can be due to the high effect of terrain elevation smoothing with the use of the Gaussian OK models.

### 7. Profiling from DTMs Created from Ground Surveying Measurements with the Use of Different OK Models

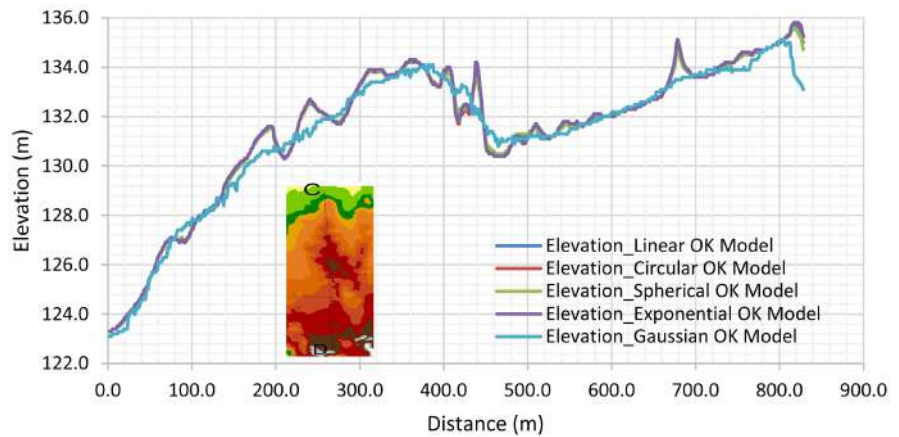
Figure 5 presents two groups of profiles depicted in Figure 5(a) and Figure 5(b) extracted from the digital elevation data with the use of the different OK

Table 4. The statistical quantities of contourline maps extracted from ground surveying measurements with the use of different OK models.

OK Model	Linear kriging	Circular kriging	Spherical kriging	Exponential kriging	Gaussian kriging
Minimum contour	117	117	117	117	117
Maximum contour	138	138	138	138	137
Count	331	376	284	374	1003
Sum	43,103	49,012	36,879	48,727	130,431
Mean contour	130	130.351	129.856	130.286	130.041
Standard Deviation	4.428	4.348	4.484	4.520	4.018



(a)



(b)

Figure 5. Profiling from ground surveying measurements with the use of different OK models. (a) Profiles across the line A-B; (b) Profiles across the Line C-D.

models namely, linear, circular, spherical, exponential, and Gaussian OK-Models. The two groups of profiles have been extracted at two different parts of the test area. From **Figure 5(a)** and **Figure 5(b)** the profiles created with the use of linear, circular, spherical, and exponential OK models run coincidentally and highly corrugated showing highly corrugated and varied terrain. However, in two groups of profiles 5(a) and 5(b), the profiles created with the use of the Gaussian model are less corrugated and tend to smooth and approximate different parts of the terrains.

## 8. Discussions and Conclusions

Gradient slope, aspect slope, profile curvature, contour curvature and drainage networks represent very important topographic parameters that are usually employed in studying a wide range of environmental and engineering applications. Topographic parameters are derived from digital elevation data through exploitation of an interpolation algorithm for creation of a continuous surface. Due to developments in computing technologies, geostatistical interpolation techniques including kriging interpolation methods have been integrated with GIS and have become strong alternatives to deterministic interpolation methods in creation of continuous surface models. Kriging interpolation approaches are geostatistical methods that take into consideration the distance and the degree of variation between the different known data points. Ordinary kriging can be performed on the discrete digital elevation data through the application of different five models namely, the linear, the circular, the spherical, the exponential and the Gaussian OK models. This research aims at extraction of different Topographic parameters from ground surveying measurements with the use of different ordinary kriging models mentioned before.

A sample of ground surveying elevation data has been employed in this study where different ordinary kriging models including the linear model, the circular model, the spherical model, the exponential model and the gaussian models have been used in extraction of the different topographic parameters from the sample of ground surveying data with use of ESRI ArcView 3.3 package with 3D analyst and Spatial analysis extensions. In this context, gradient slope maps, aspect slope maps, and hillshade maps in addition to contourline maps have been extracted from the ground surveying elevation data with the employment of the different ordinary kriging models. The following points can be drawn from visual and statistical analysis of the different extracted topographic parameters from the ground surveying data with use of the different OK models:

- There are great similarities between the slope maps from the linear, circular, spherical, and exponential OK models. These are very different from the gradient slope map from OK Gaussian regarding the different sizes and arrangement of the colour patches, referring to different tones and different textures where smooth tones and smooth textures dominate the gradient slope map from the OK Gaussian model. Also, gradient slope degradation and smoothing are considerably high in the gradient slope map from Gaussian

model compared to the slope maps from the other four OK models.

- Statistical analysis of the gradient slope maps shows that the Gaussian model records the lowest values of the mean elevations, the lowest values of the sum of slopes and the lowest value of the standard deviation of slopes which explains the less structured and highly smoothed gradient slope map obtained from the Gaussian OK model interpreted from the visual. Also, the gradient slope from the exponential model enjoys the highest values of the mean, the sum, and the standard deviation of the gradient slopes. This refers to highly structured and less smooth gradient slope maps obtained from the OK exponential models.
- The aspect slopes extracted from the ground surveying digital elevation data from linear, circular, spherical, and exponential have similar sizes and arrangement of the color patches, similar tones, and similar texture, which are very different from their correspondence in the aspect slope map from Gaussian OK model.
- Visual analysis shows strong similarities between the hillshade maps from OK linear, circular, spherical, and exponential models regarding sizes, shapes, and distribution of the color patches as well as the tones, textures and patterns in the four maps. However, the hillshade map created with the use of Gaussian model is very different. Additionally, the standard deviation of the hillshade from the Gaussian model is considerably lower than those of the hillshade from the other four models referring to the high degree of smoothing.
- Concerning the contourline maps similarities between the contourline from OK linear, circular, spherical, and exponential models regarding distribution and concentration of the contourlines. The contourline map from the Gaussian model is visually different regarding contourline shapes, distribution, and concentration.
- Profiling analysis shows that the profiles created with the use of linear, circular, spherical, and exponential OK models run coincidentally and show highly corrugated and varied terrain. However, the profiles created with the use of the Gaussian OK model are less corrugated and tend to smoothly approximate the different parts of the terrain.
- Studying more topographic parameters such as terrain curvature and drainage network can help more understanding of the behavior of the different OK models.

### **Conflicts of Interest**

The author declares no conflicts of interest regarding the publication of this paper.

### **References**

- [1] Dübel, S. and Schumann, H. (2017) Visualization of Features in 3D Terrain. *International Journal of Geo-Information*, **6**, Article 357.

- <https://doi.org/10.3390/ijgi6110357>
- [2] Tang, G. and Fayuan, L. (2006) Landform Classification of the Loess Plateau. *Proceeding of the Terrain Analysis and Digital Terrain Modelling Conference*, Nanjing, November 2006.
  - [3] Ciampalini, A., Raspini, F., Frodella, W., Bardi, F., Bianchini, S. and Moretti, S. (2016) The Effectiveness of High-Resolution LiDAR Data Combined with PSInSAR Data in Landslide Study. *Landslides*, **13**, 399-410.  
<https://doi.org/10.1007/s10346-015-0663-5>
  - [4] Liu, X., Wang, N., Shao, J. and Chu, X. (2017) An Automated Processing Algorithm for Flat Areas Resulting from DEM Filling and Interpolation. *International Journal of Geo-Information*, **6**, Article 376. <https://doi.org/10.3390/ijgi6110357>
  - [5] Maerker, M., Schillaci, C. and Kropáček, J. (2018) Morphometric Terrain Analysis to Explore Present Day Geohazards and Paleo Landscape Forms and Features in the Surroundings of the Melka Kunture Prehistoric Site, Upper Awash Valley, Central Ethiopia. *AUC Geographica*, **53**, 10-19. <https://doi.org/10.14712/23361980.2018.2>
  - [6] Zhu, A.X., Burt, J.E., Smith, M., Wang, R. and Gao, J. (2006) The Impact of Neighbourhood Size on Terrain Derivatives and Digital Soil Mapping. *Proceeding of the Terrain Analysis and Digital Terrain Modelling*, Nanjing, November 2006.
  - [7] Zhou, Q., Lees, B. and Tang, G. (2008) *Advances in Terrain Analysis*. Springer-Verlag, Berlin. <https://doi.org/10.1007/978-3-540-77800-4>
  - [8] Schillaci, C., Braun, A. and Kropaček, J. (2015) Terrain Analysis and Landform Recognition. In: Clarke, L. and Nield, J., Eds., *Geomorphological Techniques*, British Society for Geomorphology, London.
  - [9] OzTurk, D. and Kilic, F. (2016) Geostatistical Approach for Spatial Interpolation of Meteorological Data. *Annals of the Brazilian Academy of Sciences*, **88**, 2121-2136.  
<https://doi.org/10.1590/0001-3765201620150103>
  - [10] Chaplot, V., Darboux, F., Bourenane, H., Leguedois, S., Silvera, N. and Phachomphon, K. (2006) Accuracy of Interpolation Techniques for the Derivation of Digital Elevation Models in Relation to Landform Types and Data Density. *Geomorphology*, **77**, 126-141. <https://doi.org/10.1016/j.geomorph.2005.12.010>
  - [11] Malvic, T., Ivšinovic, J., Velic, J. and Rajic, R. (2019) Kriging with a Small Number of Data Points Supported by Jack-Knifing, a Case Study in the Sava Depression (Northern Croatia). *Geosciences*, **9**, Article 36.  
<https://doi.org/10.3390/geosciences9010036>
  - [12] Al-Mutairi, N., Alsahli, M., Ibrahim, M., Abou Samra, R. and El-Gammal, M. (2019) Spatial Enhancement of DEM Using Interpolation Methods: A Case Study of Kuwait's Coastal Zones. *American Journal of Remote Sensing*, **7**, 5-12.  
<https://doi.org/10.11648/j.ajrs.20190701.12>
  - [13] ESRI (2002) *ArcGIS 9: Using ArcGIS Spatial Analyst*.
  - [14] ESRI (2003) *ArcGIS 9: Using ArcGIS Geostatistical Analyst*.
  - [15] Jiao, Y., Zhang, F., Huang, Q., Liu, X. and Li, L. (2023) Analysis of Interpolation Methods in the Validation of Backscattering Coefficient Products. *Sensors*, **23**, Article 469. <https://doi.org/10.3390/s23010469>
  - [16] Ryu, J.S., Cha, M.K., Lee, T.H. and Choi, D.H. (2002) Kriging Interpolation Methods in Geostatistics and DA CE Model. *KSME International Journal*, **16**, 619-632.  
<https://doi.org/10.1007/BF03184811>
  - [17] Taharin, M.R. and Roslee, R. (2021) The Application of Semi Variogram and Ordinary Kriging in Determining the Clay Percentage Distribution in Hilly Area of Sa-

- bah, Malaysia. *International Journal of Design & Nature and Eco-Dynamics*, **16**, 525-530. <https://doi.org/10.18280/ijdne.160506>
- [18] Dressler, M. (2009) Art of Surface Interpolation. Kunštát. <https://api.semanticscholar.org/CorpusID:18798556>
- [19] Gumus, K. and Sen, A. (2013) Comparison of Spatial Interpolation Methods and Multi-Layer Neural Networks for Different Point Distributions on a Digital Elevation Model. *Geodetski Vestnik*, **57**, 523-543. <https://doi.org/10.15292/geodetski-vestnik.2013.03.523-543>
- [20] Xing, Y., de Gier, A., Zhang, J. and Wang, L. (2010) An Improved Method for Estimating Forest Canopy Height Using ICESat-GLAS Full Waveform Data over Sloping Terrain: A Case Study in Changbai Mountains, China. *International Journal of Applied Earth Observation and Geoinformation*, **12**, 385-392. <https://doi.org/10.1016/j.jag.2010.04.010>
- [21] Jensen, J. (2015) Introductory Digital Image Processing: A Remote Sensing Perspective. Fourth Edition, Pearson Education, London.
- [22] Lillesand, T.M. and Keifer, R.W. (2015) Remote Sensing and Image Interpretation. Fourth Edition, John Wiley & Sons, New York.
- [23] Kennelly, P.J. (2008) Terrain Maps Displaying Hill-Shading with Curvature. *Geomorphology*, **102**, 567-577. <https://doi.org/10.1016/j.geomorph.2008.05.046>